Single-ion and pair-interaction potentials near simple metal surfaces

R. N. Barnett, R. G. Barrera,* C. L. Cleveland, and Uzi Landman
School of Physics, Georgia Institute of Technology, Atlanta, Georgia 30332
(Received 20 August 1982)

We present a model for semi-infinite simple metals which does not require crystalline order or a single species, and thus is applicable to problems of defect energetics near the surface and random-alloy surfaces as well as ideal metal surfaces. The formulation is based on the use of ionic psuedopotentials and linear-response theory. An expression for the total energy is obtained which depends explicitly on ionic species and position. This expression is decomposed into a density-dependent term and single-ion and ionic pair-interaction potential terms. The single-ion potentials oscillate about a constant bulk value, with the magnitude of the oscillation decreasing rapidly away from the surface. The interaction between pairs of ions near the surface is shown to be a noncentral force interaction which differs significantly from the central-force bulk pair potential. The effect of quantum interference in the response of the semi-infinite electron gas to the ions is seen in both the single-ion and the pair-interaction potentials. Results are presented for the simple metals sodium, potassium, and rubidium.

I. INTRODUCTION

Fundamental investigations of certain physical properties of solid materials such as crystallographic structure, dynamics, and defect energetics (formation and migration) require detailed knowledge of, and the ability to calculate, the total energy or total-energy differences for various configurations. The total energy of metals, simple metals in particular, contains contributions of different origins, e.g., terms in the electronic energy which are density dependent (independent of the location of atoms) and terms which depend on the spatial arrangement of the atoms.[1] It is important to recognize that the dominant factors underlying various physical properties may relate to terms in the total energy which are of different origins. Thus, for example, the determination of crystallographic structure requires a minimization of the total energy including the contribution which is only density dependent[2] while the dominant contributions in studies of vibrations of bulk metals come from those terms which depend on the interatomic position vectors.[1,3] Determination of the surface atomic arrangement (relaxation and reconstruction) may require, in addition, terms which depend on the positions of individual atoms relative to ideal (truncated bulk) crystal planes.[4]

Essential to the construction of theoretical treatments of the properties of perfect bulk crystals is the translational invariance of the lattice. The lack of translational symmetry causes major difficulties in the exploration of properties of imperfect crystals, and theoretical formulations which can provide quantitative estimates of structure, energetics, and dynamics of real (imperfect) materials, while most desirable, are less abundant. Material surfaces in the ideal case possess two-dimensional translational symmetry parallel to the surface plane but lack translational symmetry along the surface normal. Consequently, theoretical treatments of surface properties are complex and require new formulations or adaptations of bulk methods with major modifications. Among the formalisms which have greatly enhanced our understanding of surfaces are density-functional-based techniques,[5,6] methods which employ real-space or mixed representations (recursion techniques,[7] Green's functions[8]), and surface band-structure computations[9] (slab and supercell techniques).

While significant progress in the theory of the electronic structure of ideal metallic surfaces and with ordered arrays of adsorbates has been achieved, calculations which employ minimization of the total energy yielding surface structural information,[4,10–12] calculations of force constants for use in surface vibrational studies, and evaluation of interaction potentials for use in molecular-dynamics and Monte Carlo simulations are in their infancy.[13,14] The introduction of single or randomly arranged defects to the surface region compounds the complexity since the lack of translational invariance is exhibited by both components of the system. Thus traditional band-structure calculations are not applicable and application of the density-functional method becomes difficult, involving approximate perturbative (most often first-order[15]) treatments, or it may entail a reduction in the dimensionality through averaging over the ionic potentials in layers.

The purpose of this article is to develop a theoretical method for simple (*sp* bonded) metals which retains the three-dimensional character of the system, maintains the essential features of the electronic structure, and allows (a) systematic investigations of ionic potentials (effective pair potentials and single-ion potentials in the surface region), (b) studies of surface structure (relaxation and reconstruction), (c) analysis of the energetics of single and randomly distributed defects, and (d) studies of surface segregation phenomena[16] in alloys (layer concentration profiles) via minimization of the surface free energy. An application of the formulation developed here to the prediction of the relaxed surface structure of the low-index faces of Na and Al, yielding good *quantitative* agreement with available experimental results, has been reported.[17] A detailed description of the surface relaxation calculation and a discussion of the results are given in the second paper of this series.[18a] Impurity and vacancy formation energies and surface segregation in alloys have been reported[18b] by us

and will be treated in forthcoming publications.

To enable us to perform the studies listed above we need first to obtain an expression for the total energy of a semi-infinite metal which depends explicitly on the atomic species and their positions. Pseudopotentials, often in conjunction with linear-response theory, have been instrumental in investigations of bulk metal systems.[1] In particular, the application of local model pseudopotentials has yielded effective interaction potentials which have been well tested in studies of vibrations,[19–22] elastic properties and vacancy formation energy and volume,[22–26] and in molecular-dynamics simulations.[27–29]

In Sec. II of this paper we present the general formulation and obtain an expression for the total energy of a semi-infinte simple metal. This total-energy expression is most general in that it does not require crystalline order or a single species. The formulation employs local model pseudopotentials embedded in a semi-infinite interacting electron gas. The response of the electron gas to an embedded ion is obtained through the solution of a single one-dimensional integral equation and involves the use of a linear-response model applicable to the semi-infinte system. A decomposition of the total energy into (a) a density-dependent term, (b) terms which depend on the coordinates of a single ion, and (c) terms which depend jointly on the coordinates of pairs of ions is accomplished. In Sec. III we apply the theory to the calculation of single-ion and pair-interaction potentials in the surface region of simple metals. We find that near the surface the single-ion potentials oscillate about the (constant) bulk values and that the pair-interaction potentials are anisotropic and differ significantly from the bulk interaction.

II. TOTAL ENERGY OF SEMI-INFINITE SIMPLE METALS

A. Total-energy expressions

The metal surface system which we wish to study is conveniently represented by a semi-infinite interacting electron gas in the presence of a neutralizing positive background (jellium model), to which we add the appropriate ionic potentials. The Hamiltonian for the electrons is written as

$$H=H^0+\sum_i w_i \ . \tag{1}$$

H^0 is the many-body Hamiltonian of the interacting electron-jellium system,

$$H^0=T+V_{ee}+V_+ \ , \tag{2}$$

where T and V_{ee} are the electron kinetic energy and electron-electron interaction operators, respectively, and $V_+(\vec{r})$ is the potential due to the positive background. The potentials associated with individual ions, w_i, are given by

$$w_i(\vec{r})=V_p(\beta_i;|\vec{r}-\vec{r}_i|)-N^{-1}Z(\beta_i)V_+(\vec{r}) \ , \tag{3}$$

where $V_p(\beta_i;|\vec{r}-\vec{r}_i|)$ and $Z(\beta_i)$ are the bare ionic pseudopotential and valence charge, respectively, of the ion of species β_i located at position $\vec{r}_i$, and $N=\sum_i Z(\beta_i)$. The second term in the right-hand side (rhs) of Eq. (1) subtracts the potential due to the jellium background and adds the potential due to an arrangement of ions represented by local model pseudopotentials.

In this study we employ pseudopotentials of the simplified Heine-Abarenkov form,

$$V_p(\beta;r)=\begin{cases} -Z(\beta)e^2/r, & r\geq r_c(\beta) \quad (4a) \\ -Z(\beta)u_c(\beta)e^2/r_c(\beta), & r<r_c(\beta) \quad (4b) \end{cases}$$

where the core radius and level parameters, $r_c(\beta)$ and $u_c(\beta)$, are chosen to fit bulk properties (lattice constant and bulk modulus[25]) of the pure species β.

The ground-state energy E_0 and electron density $\rho^0(\vec{r})$ of the jellium system described by H^0 [Eq. (2)] is given in a seminal study by Lang and Kohn.[30] With the use of the coupling-constant integration method and assuming linear response, the total energy E_T of the semi-infinite metal is given by

$$E_T=E^0+\sum_i\int d^3r\,\rho^0(\vec{r})w_i(\vec{r}) + \tfrac{1}{2}\sum_{i,j}\int d^3r\,\rho_i(\vec{r})w_j(\vec{r})+E_M \ , \tag{5}$$

where $\rho_i(\vec{r})$ is the electron density induced by the potential $w_i(\vec{r})$, and E_M is the Madelung energy of the ionic system. The second term in Eq. (5) is a first-order correction due to the replacement of the positive background by discrete ions, and the third term is second order in w_i, usually called the band-structure (BS) energy $E_{\rm BS}$.

B. Screening

The major task in obtaining the total energy, Eq. (5), for an arbitrary arrangement of ions is to obtain a self-consistent solution for the induced, or screening, electron density $\rho_i(\vec{r})$. We use linear-response theory, yielding a pair of coupled integral equations,

$$\rho_i(\vec{r})=\int d^3r'\alpha_0(\vec{r},\vec{r}')[w_i(\vec{r}')+\phi_i(\vec{r}')] \ , \tag{6a}$$

$$\phi_i(\vec{r})=\int d^3r'g(\vec{r},\vec{r}')v_C(|\vec{r}-\vec{r}'|)\rho_i(\vec{r}') \ , \tag{6b}$$

where $\alpha_0(\vec{r},\vec{r}')$ is the random-phase-approximation (RPA) response function (polarizability). $\phi_i(\vec{r})$ is the effective potential due to the electron density $\rho_i(\vec{r})$, which includes exchange and correlation effects via the function $g(\vec{r},\vec{r}')=1-G(\vec{r},\vec{r}')$, and $v_C(\vec{r})=e^2/r$ is the Coulomb interaction. $G(\vec{r},\vec{r}')$ is a local-field correction, related to the electron pair correlation function of the jellium system, which takes into account short-range correlations arising from both Coulomb and exchange effects.[31]

Translational invariance parallel to the surface requires that

$$\alpha_0(\vec{r},\vec{r}')=\alpha_0(|\vec{R}-\vec{R}'|;z,z')$$

and

$$g(\vec{r},\vec{r}')=g(|\vec{R}-\vec{R}'|;z,z') \ ,$$

with $\vec{r}=(\vec{R},z)$ (here and in the following, upper-case letters denote two-dimensional vector, parallel to the surface). An evaluation of the response function requires knowledge of the single-particle wave functions and energy eigenvalues of the interacting electron-jellium system. These are of the form

$$\Psi_{\vec{K},\kappa}(\vec{r})=\Omega^{-1/2}e^{i\vec{K}\cdot\vec{R}}\psi_\kappa(z)\,,$$
$$E(\vec{K},\kappa)=\hbar^2K^2/2m+\epsilon_\kappa\,, \tag{7}$$

respectively, where $\Omega=N\Omega_0$ is the volume of the semi-infinite metal (Ω_0 is the volume per electron). The response function (retarded polarizability) is given in a mixed representation by

$$\alpha_0(Q;z,z')=2\Omega^{-2/3}\sum_{\kappa,\kappa'}\mathscr{L}(Q;\kappa,\kappa')\psi^*_\kappa(z)\psi_{\kappa'}(z)\times\psi^*_{\kappa'}(z')\psi_\kappa(z')\,, \tag{8a}$$

$$\mathscr{L}(Q;\kappa,\kappa')=\Omega^{-2/3}\sum_{\vec{K}}\frac{f(\vec{K}-\vec{Q}/2,\kappa)-f(\vec{K}+\vec{Q}/2,\kappa')}{E(\vec{K}-\vec{Q}/2,\kappa)-E(\vec{K}+\vec{Q}/2,\kappa')}\,, \tag{8b}$$

where $f(\vec{K},\kappa)$ is the Fermi-Dirac distribution function, and $\mathscr{L}(Q;\kappa,\kappa')$ is the two-dimensional RPA response function.[32]

To obtain the response function, Eq. (8a), we must either numerically evaluate the single-particle wave functions, $\psi_\kappa(z)$, or use an approximate analytical form. Our choice is to use the wave functions of a noninteracting electron gas confined to the half-space ($z>0$) by an infinite barrier.[32–35] This choice is dictated primarily by analytical convenience. Other choices are possible[36]; for instance, one could solve for the single-particle wave functions resulting from the potential due to the Lang-Kohn electron density plus the positive background. However, the increased complexity of such choices results in formulations which are impractical or impossible to use in a systematic study which retains the three-dimensional character of the system. Lert and Weare[32] have used the infinite barrier response model to calculate the electron density at the Na(100) surface and report that comparison of their results with the self-consistent nonlinear results of Appelbaum and Hamann[37] indicates the joint validity of the linear approximation and the infinite barrier response model. The overconfinement of the electrons outside the jellium surface in this model might contribute to the surface energy. However, we are interested primarily in *total-energy differences* resulting from a rearrangement of the ions or a change in species of some ions, and contributions due to overconfinement are expected to be of less significance due to cancellation. In addition, the success of this response model in predicting the relaxed surface structure of simple metals[17,18(a)] lends some *a posteriori* validation to the approximation.

The basis-set wave functions and energies associated with the infinite barrier response model are given by

$$\psi_\kappa(z)=\sin(\kappa z)\Theta(z)\,, \tag{9a}$$

$$\epsilon_\kappa=\frac{\hbar^2}{2m}\kappa^2\,, \tag{9b}$$

where Θ is the Heaviside unit step function. The surface barrier is located at $z=0$ and the jellium edge position, determined by charge neutrality, is $z_0=3\pi/8k_F$ (Ref. 38); the layers of an unrelaxed crystal will be located at $z_n=z_0+(n-\frac{1}{2})D$, where $n=1$ for the surface layer and D is the layer spacing. Substituting Eqs. (9) into Eq. (8a) gives the infinite barrier model response function

$$\alpha_0(Q;z,z')=2\Omega^{-2/3}\sum_{\kappa,\kappa'}\mathscr{L}(Q;\kappa,\kappa')\sin(\kappa z)\sin(\kappa z')\times\sin(\kappa' z)\sin(\kappa' z')\Theta(z)\Theta(z')\,. \tag{10}$$

The analytical convenience of this response model is due to the vanishing of $\alpha_0(Q;z,z')$ if either $z\le 0$ or $z'\le 0$, or both; thus it is possible to symmetrize the problem by reflecting across the $z=0$ plane. We define symmetrized quantities $\rho_{is}(\vec{r})$, $w_{is}(\vec{r})$, and $\phi_{is}(\vec{r})$, and their three-dimensional Fourier transforms, by

$$\rho_{is}(\vec{r})=\rho_i(R,|z|)\,, \tag{11a}$$

$$\rho_{is}(\vec{q})=\int d^3r\,e^{i\vec{q}\cdot\vec{r}}\rho_{is}(\vec{r})\,, \tag{11b}$$

etc. Using these definitions, we obtain from Eq. (6a), after some manipulation, an equation in reciprocal space for the induced electron density in the symmetrized system (see Appendix A),

$$\rho_{is}(\vec{q})=\alpha_0(q)[w_{is}(\vec{q})+\phi_{is}(\vec{q})]-\pi^{-1}\int d\kappa\,\mathscr{L}(Q;\kappa+q_z/2,\kappa-q_z/2)\times[w_{is}(Q,2\kappa)+\phi_{is}(Q,2\kappa)]\,. \tag{12}$$

Here $\alpha_0(q)$ is the three-dimensional Fourier transform of the polarizability of an infinite electron gas as given by Lindhard,[39]

$$\alpha_0(q)=\pi^{-1}\int d\kappa\,\mathscr{L}(Q;\kappa+q_z/2,\kappa-q_z/2)\,. \tag{13}$$

Integrating Eq. (12) over q_z results in a useful sum rule,

$$\int dq_z\rho_{is}(\vec{q})=0\,, \tag{14}$$

expressing the fact that the induced density is zero at $z=0$.

The equation for the self-consistent effective potential, Eq. (6b), takes, in the symmetrized system, the form

$$\phi_{is}(\vec{q})=\int d^3r\,e^{i\vec{q}\cdot\vec{r}}\int d^3r'g(|\vec{R}-\vec{R}'|;z,z')\times v_C(|\vec{r}-\vec{r}'|)\rho_{is}(\vec{r}')\times[1-\Theta(z)\Theta(-z')-\Theta(-z)\Theta(z')]\,. \tag{15}$$

In order to simplify Eq. (15), and to allow the solution of the coupled integral Eqs. (12) and (15) to be reduced to the solution of a single one-dimensional integral equation, we will assume that $g(|\vec{R}-\vec{R}'|;z,z')$ can be adequately approximated by

$$g(|\vec{R}-\vec{R}'|;z,z')=1-G(|\vec{r}-\vec{r}'|)$$

where $G(|\vec{r}-\vec{r}'|)$ is the local-field correction evaluated for the bulk electron density. This approximation may be

justified for several reasons: (a) It introduces only second-order errors, (b) $G(\vec{r},\vec{r}')$ does not depend sensitively on the local density, and (c) experience with other systems indicates that anisotropic or inhomogeneous corrections in condensed systems are usually small.[40]

Employing the above form of $g(\vec{r},\vec{r}')$, Eq. (15) becomes (see Appendix B)

$$\phi_{is}(\vec{q})=g(q)v_C(q)\rho_{is}(\vec{q})+v_C(q)\sigma_i(Q)+X_i(\vec{q}) , \quad (16)$$

where $g(q)$ is the Fourier transform of $g(r)$ evaluated for the bulk electron density. We use the analytical fit

$$g(q)=1-A[1-\exp(-Bq^2/k_F^2)]$$

given by Singwi *et al.*[31] $v_C(q)=4\pi e^2/q^2$ is the Fourier-transformed Coulomb potential. $v_C(q)\sigma_i(Q)$ and $X_i(\vec{q})$ are functions which subtract the interaction of the induced electron density with its image in the symmetrized system. The Coulomb interaction between the induced electron density and its image is canceled by

$$\sigma_i(Q)=-(Q/2\pi)\int dq_z[\rho_{is}(\vec{q})/q^2] , \quad (17)$$

which can be regarded as a fictitious surface electron density, and

$$X_i(\vec{q})=-\int d^3r\, e^{i\vec{q}\cdot\vec{r}}\int d^3r'[g(|\vec{r}-\vec{r}'|)-1] \times v_C(|\vec{r}-\vec{r}'|)\rho_{is}(\vec{r}') \times[\Theta(z)\Theta(-z') +\Theta(-z)\Theta(z')] \quad (18)$$

subtracts the exchange-correlation potential due to the image electron density. Since the local-field correlation function $G(r)=1-g(r)$ is short ranged, and since the induced electron density $\rho_{is}(\vec{r}')$ vanishes as $z\to 0$, $X_i(\vec{q})$ can be neglected. *A posteriori* validation of this approximation is provided by the observation that the sum rule, Eq. (14) (which was derived with no approximation), is satisfied by our numerical results when $X_i(\vec{q})$ is neglected.

The coupled integral equations, Eq. (12) and Eqs. (16)–(18), can be decoupled by setting

$$\rho_{is}(\vec{q})=\alpha_0(q)[w_{is}(\vec{q})+v_C(q)\sigma_i(Q)]/\epsilon(q) +[u_i(\vec{q})+u_\sigma(\vec{q})\sigma_i(Q)]/[g(q)v_C(q)] , \quad (19)$$

where

$$\epsilon(q)=1-g(q)v_C(q)\alpha_0(q) \quad (20)$$

is the (bulk) electron dielectric function, and $u_i(\vec{q})$ and $u_\sigma(\vec{q})$ are to be determined. Combining Eqs. (12), (16), and (19), and requiring that the coefficients of $\sigma_i(Q)$ cancel, results in a single one-dimensional integral equation for $u_i(\vec{q})$,

$$u_i(\vec{q})=-[g(q)v_C(q)/\epsilon(q)]\pi^{-1} \times\int d\kappa\,\mathscr{L}(Q;\kappa+q_z/2,\kappa-q_z/2) \times[u_i(\vec{q}')+w_{is}(\vec{q}')/\epsilon(q')] , \quad (21)$$

where $\vec{q}'=(\vec{Q},2\kappa)$, and in a similar equation for $u_\sigma(\vec{q})$ in which $w_{is}(\vec{q}')$ is replaced by $v_C(q')$ in the integral. These equations are solved numerically by successive iteration. Since $\sigma_i(Q)$ is independent of q_z, substituting Eq. (19) into Eq. (17) yields immediately an expression for $\sigma_i(Q)$ in terms of $u_i(\vec{q})$ and $u_\sigma(\vec{q})$.

Note that in Eq. (19) the first term on the rhs describes the bulk response to the potential $[w_{is}(\vec{q})+v_C(q)\sigma_i(Q)]$. It is apparent that $u_i(\vec{q})$ and $u_\sigma(\vec{q})$ in the second term contain the effects of quantum interference associated with the semi-infinite bounded electron gas. These quantum interference effects become small, as does $\sigma_i(Q\neq 0)$ (the nonvanishing contributions to the fictitious surface electron density due to w_i), as the ion position $\vec{r}_i$ moves further from the surface, and bulk screening is obtained for ions far from the surface. The semiclassical limit ($\hbar\to 0$ with $\hbar k_F=$ const) amounts to neglect of these quantum interference terms.[33] However, in this limit the position of the jellium edge is at $z_0=0$ and, therefore, there is no response beyond the jellium edge.

C. Total-energy decomposition

The total energy, Eq. (5), can be decomposed into a term $U^{(0)}(\Omega_0)$ which depends only on the average electron density of the semi-infinite metal, terms $U^{(1)}(\Omega_0;\beta_i,z_i)$ which depend on the species and the positions of individual ions relative to the surface, and terms $U^{(2)}(\Omega_0;\beta_i,\vec{r}_i;\beta_j,\vec{r}_j)$ which depend on the species and the coordinates of pairs of ions; thus the total-energy expression becomes

$$E_T=U^{(0)}(\Omega_0)+\sum_i U^{(1)}(\Omega_0;\beta_i,z_i) +\tfrac{1}{2}\sum_{i,j}U^{(2)}(\Omega_0;\beta_i,\vec{r}_i;\beta_j,\vec{r}_j) . \quad (22)$$

The purpose of this section is to show that this decomposition is possible and to derive the expressions for the single-ion and pair-interaction potentials, $U^{(1)}$ and $U^{(2)}$. It should be noted that this decomposition is not particularly useful in performing most calculations since it is usually simpler to take advantage of the geometry specific to the problem and do the calculation in reciprocal space. However, we can gain some insight into how ionic interactions differ at the surface and in the bulk, and the decomposition may be useful in, for instance, molecular-dynamics and Monte Carlo simulations.

We begin by separating $w_i(\vec{r})$ and $\rho_i(\vec{r})$ into ionic pseudopotential, $\tilde{w}_i$ and $\tilde{\rho}_i$, and positive background, V_P and ρ_+, parts:

$$w_i(\vec{r})=Z_i[\tilde{w}_i(\vec{r})-(\Omega_0/\Omega)V_+(\vec{r})] \quad (23a)$$

and

$$\rho_i(\vec{r})=Z_i[\tilde{\rho}_i(\vec{r})-(\Omega_0/\Omega)P_+(\vec{r})] , \quad (23b)$$

where for notational convenience we have defined

$$\tilde{w}_i(\vec{r})=Z_i^{-1}V_p(\beta_i;|\vec{r}-\vec{r}_i|)$$

[see Eqs. (3) and (4)] and $Z_i=Z(\beta_i)$. In defining the Fourier transforms of the symmetrized quantities $\tilde{w}_{is}(\vec{r})$ and $\tilde{\rho}_{is}(\vec{r})$ we shift the ions to the origin in the $x-y$ plane,

$$\tilde{w}_{is}(\vec{q})=\int d^2R\, e^{i\vec{Q}\cdot(\vec{R}-\vec{R}_i)}\int dz\cos(q_z z)\tilde{w}_{is}(\vec{r})\ , \tag{24}$$

etc. The reciprocal-space representations of the potentials $\tilde{w}_{is}(\vec{q})$ and $V_{+s}(\vec{q})$ are given by (see Appendix C)

$$\tilde{w}_{is}(\vec{q})=2Z_i^{-1}V_p(\beta_i;q)\cos(q_z z_i)+v_C(q)e^{-Qz_i}\ , \tag{25}$$

where $V_p(\beta_i;q)$ is the Fourier transform of $V_p(\beta_i;r)$, and

$$V_{+s}(\vec{q})=(2\pi)^2\Omega_0^{-2/3}\delta(\vec{Q})v_{+s}(q_z)\ , \tag{26a}$$

where

$$v_{+s}(q_z)=-2\Omega_0^{-1/3}v_C(q_z)[\pi\delta(q_z)-\sin(q_z z_0)/q_z]\ . \tag{26b}$$

The induced electron densities $\tilde{\rho}_{is}(\vec{q})$ and $\rho_{+s}(q_z)$ are obtained as before using $\tilde{w}_{is}(\vec{q})$ or $v_{+s}(q_z)$ with $\vec{Q}=0$, respectively, in place of $w_{is}(\vec{q})$ in Eq. (12). Finally, we define $\tilde{\sigma}_i(Q)$ by using $\tilde{\rho}_{is}(\vec{q})$ in place of $\rho_{is}(\vec{q})$ in Eq. (17). With this definition, $\sigma_i(Q)$ is given by

$$\sigma_i(Q)=Z_i[\tilde{\sigma}_i(Q)+(2\pi)^2\Omega^{-2/3}\delta(\vec{Q})]\ . \tag{27}$$

It can be shown [see Eq. (B7)] that $\lim_{Q\to 0}\tilde{\sigma}_i(Q)=-1$, in agreement with our numerical results.

The total energy, Eq. (5), expressed in terms of the reciprocal-space functions $w_{is}(\vec{q})$ and $\rho_{is}(\vec{q})$, is

$$E_T=E_0+\sum_i\int d^3r\,\rho^0(\vec{r})w_i(\vec{r})+\tfrac{1}{4}\sum_{i,j}(2\pi)^{-3}\int d^3q\,\rho_{is}(\vec{q})w_{js}(\vec{q})+E_M\ . \tag{28}$$

The factor of $\frac{1}{4}$ instead of $\frac{1}{2}$ in the third term (the band-structure energy) is due to the symmetrization of the system (in effect we have two noninteracting semi-infinite systems). Substitution of Eqs. (23)–(26) into Eq. (28) yields, after some algebra,

$$\begin{aligned}E_T=E_0&-\int d^3r\,\rho^0(\vec{r})V_+(\vec{r})+\tfrac{1}{4}(\Omega/\Omega_0^2)^{2/3}(2\pi)^{-1}\int dq_z\rho_{+s}(q_z)v_{+s}(q_z)+\sum_i Z_i\int d^3r\,\rho^0(\vec{r})\tilde{w}_i(\vec{r})\\&-\tfrac{1}{4}\Omega_0^{-2/3}\sum_i Z_i(2\pi)^{-1}\int dq_z[\tilde{\rho}_{is}(0,q_z)v_{+s}(q_z)+\rho_{+s}(q_z)\tilde{w}_{is}(0,q_z)]\\&+\tfrac{1}{4}\sum_i Z_i^2(2\pi)^{-3}\int d^3q\,\tilde{\rho}_{is}(\vec{q})\tilde{w}_{is}(\vec{q})+\tfrac{1}{4}{\sum_{i,j}}'Z_iZ_j(2\pi)^{-3}\int d^3q\tilde{\rho}_{is}(\vec{q})\tilde{w}_{js}(\vec{q})e^{i\vec{Q}\cdot(\vec{R}_i-\vec{R}_j)}+E_M\ ,\end{aligned} \tag{29}$$

where the primed sum $\sum'_{i,j}$ omits the $i=j$ terms.

The only terms in Eq. (29) which depend on the coordinates of more than one ion are the last two terms. Thus we define the pair-interaction potential $U^{(2)}$ to be

$$U^{(2)}(\Omega_0;\beta_i,\vec{r}_i;\beta_j,\vec{r}_j)=Z_iZ_j/|\vec{r}_i-\vec{r}_j|+\tfrac{1}{4}Z_iZ_j(2\pi)^{-3}\int d^3q[\tilde{\rho}_{is}(\vec{q})\tilde{w}_{js}(\vec{q})+\tilde{\rho}_{js}(\vec{q})\tilde{w}_{is}(\vec{q})]e^{i\vec{Q}\cdot(\vec{R}_i-\vec{R}_j)}\ . \tag{30}$$

Since the two-dimensional (2D) vector $\vec{R}_i$ does not appear in the definition of $\tilde{w}_{is}(\vec{q})$ or $\tilde{\rho}_{is}(\vec{q})$, it is evident that the pair-interaction potential depends on $|\vec{R}_i-\vec{R}_j|$, the magnitude of the distance between two ions parallel to the surface. However, this pair-interaction potential depends on the z coordinates of the two ions separately rather than just on $|z_i-z_j|$, i.e.,

$$U^{(2)}(\Omega_0;\beta_i,\vec{r}_i;\beta_j,\vec{r}_j)=U^{(2)}(\Omega_0;|\vec{R}_i-\vec{R}_j|;\beta_i,z_i;\beta_j,z_j)\ .$$

For this reason $U^{(2)}$ is not a pair-potential in the usual sense but can be regarded as a three-body potential, where the third body is the electron-jellium system described by H^0, Eq. (2).

The single-ion potential is contained in the fourth, fifth, and sixth terms on the rhs of Eq. (29) since these terms depend on the z coordinate of a single ion,

$$\begin{aligned}U^{(1)}(\Omega_0;\beta_i z_i)=Z_i\int d^3r\,\rho^0(\vec{r})\tilde{w}_i(\vec{r})&-\tfrac{1}{4}\Omega_0^{-2/3}Z_i(2\pi)^{-1}\int dq_z[\tilde{\rho}_{is}(0,q_z)v_{+s}(q_z)+\rho_{+s}(q_z)\tilde{w}_{is}(0,q_z)]\\&+\tfrac{1}{4}Z_i^2(2\pi)^{-3}\int d^3q\,\tilde{\rho}_{is}(\vec{q})\tilde{w}_{is}(\vec{q})\ .\end{aligned} \tag{31}$$

The physical origins of the three terms on the rhs of Eq. (31) are, respectively, (i) the interaction of the bare ion with the unperturbed electron density, (ii) the interaction of the ion and the (subtracted) positive background density through their screening electron densities, and (iii) the interaction of the ion with its own screening electron density. The terms (i) and (ii) taken separately are divergent since the system is semi-infinite, but the sum of the two is finite.

In order to evaluate Eq. (31) the direct interaction of the ion with the positive background is added to the first term and subtracted from the second. The expression for this ion-positive background interaction energy is

$$\begin{aligned}&-\int d^3r\,P^J(\vec{r})Z_i\tilde{w}_i(\vec{r})\\&\quad=-\tfrac{1}{2}\Omega^{-2/3}Z_i(2\pi)^{-1}\int dq_z[\rho_{is}^I(0,q_z)v_{+s}(q_z)]\\&\quad=-\tfrac{1}{2}\Omega^{-2/3}Z_i(2\pi)^{-1}\int dq_z[\rho_s^J(q_z)\tilde{w}_{is}(0,q_z)]\ ,\end{aligned} \tag{32}$$

where $P^J(\vec{r})=\Omega_0^{-1}\Theta(z-z_0)$ is the positive background (jellium) density, with symmetrized Fourier transform

$$P_s^J(\vec{q})=(2\pi)^2\Omega_0^{-2/3}\delta(\vec{Q})\rho_s^J(q_z)\ ,$$

and

TABLE I. Parameters used in the calculations: $r_s=(3\Omega_0/4\pi)^{1/3}$ is the electron density parameter, r_c and u_c are the pseudopotential core radius and depth (Ref. 25) [see Eq. (4)], and A and B are the parameters in the local-field correction $G(q)$ Ref. 30 [see Eq. (6)].

Metal	r_s	r_c	u_c	A	B
Na	$3.931a_0$	$2.076a_0$	0.3079	0.9942	0.2631
K	$4.862a_0$	$3.033a_0$	0.5723	1.0119	0.2406
Rb	$5.197a_0$	$3.551a_0$	0.7273	1.0161	0.2337

$$Z_i\rho_{is}^I(\vec{q})=v_C(q)^{-1}2V_p(\beta_i;q)\cos(q_z z_i)$$

is the positive density which gives rise to the ionic pseudopotential [see Eq. (C5)]. With the use of Eq. (32) as discussed above, the expression for the single-ion potential becomes

$$U^{(1)}(\Omega_0;\beta_i,z_i)=E_S+E_H+E_{\rm BS}^0 , \tag{33}$$

where

$$E_S=\tfrac{1}{4}Z_i^2(2\pi)^{-3}\int d^3q\,\tilde{\rho}_{is}(\vec{q})\tilde{w}_{is}(\vec{q}) , \tag{34a}$$

$$E_H=Z_i\int d^3r[\rho^0(\vec{r})-P^J(\vec{r})]\tilde{w}_{is}(\vec{r}) , \tag{34b}$$

and

$$E_{\rm BS}^0=\tfrac{1}{4}\Omega_0^{-2/3}Z_i(2\pi)^{-1}\times\int dq_z\{[\rho_{is}^I(0,q_z)-\tilde{\rho}_{is}(0,q_z)]v_{+s}(q_z)+[\rho_s^J(q_z)-\rho_{+s}(q_z)]\tilde{w}_{is}(0,q_z)\} . \tag{34c}$$

We remind the reader that $\tilde{\rho}_{is}$ and ρ_{+s} are *induced* electron densities corresponding to the potentials $\tilde{w}_{is}$ and v_{+s}, respectively [Eqs. (25) and (26)], which are in turn the potentials due to the densities ρ_{is}^I and ρ_s^J which represent the ions and positive background, respectively. Having described in this section the physical model and derived the expressions needed for the evaluation of the total energy and its decomposition into density, single-ion, and pair-interaction potentials, we turn now to a discussion of results for the single-ion and pair-interaction potentials.

III. RESULTS AND DISCUSSION

In this section the theory developed in Sec. II is employed in a systematic study of the single-ion and ion pair-interaction potentials in the simple metals Na, K, and Rb. The values of the bulk electron density parameter r_s, the pseudopotential core radius and depth [Eq. (4)] r_c and u_c,[25] and the parameters A and B in the analytical fit to the local-field (exchange-correlation) correction $G(q)$ (Ref. 31) which were used in the calculations are given in Table I.

In general, the practice of determining model pseudopotential parameters is guided by the adequacy of the fit between calculated and measured material properties. When treating metal surfaces, and possible structural relaxations, it is essential to use a model which yields the correct bulk lattice constant and reproduces the elastic properties of the bulk. In addition, if the model is to be applied to alloys (heats of formation, surface segregation, etc.) it is of utmost importance that the model also yield the correct total energy, and thus the cohesive energy, of the bulk pure species. The pseudopotential parameters, r_c and u_c, which we employ were determined by Popovic *et al.*[25] to reproduce the experimental values of the bulk modulus and equilibrium lattice constant. These authors used the pseudopotentials, and the local-field correction of Singwi *et al.*[31], in calculations of vacancy formation energies and volumes for the alkali metals and Al, obtaining results in good agreement with experimental values. We have calculated the cohesive energy of Na, K, and Rb using the pseudopotentials and find that the calculated and experimental values agree to within less than 0.3% in each case (experimental values are summarized in Ref. 20). To our knowledge these pseudopotentials have not been used in lattice-dynamics calculations; nevertheless, the bulk pair-potentials which we obtain are similar (in terms of loca-

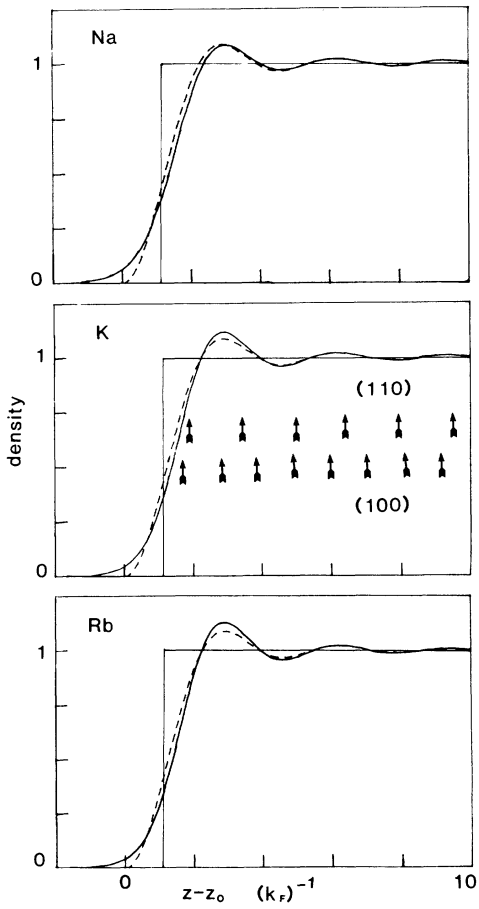

FIG. 1. Electron densities $\Omega_0\rho^0(z)$ for Na, K, and Rb. The Lang-Kohn (Ref. 30) densities are shown as solid curves and the dashed curves are the infinite barrier noninteracting electron density. The truncated bulk density is also shown as a solid line, and the (100) and (110) layer positions are indicated by arrows.

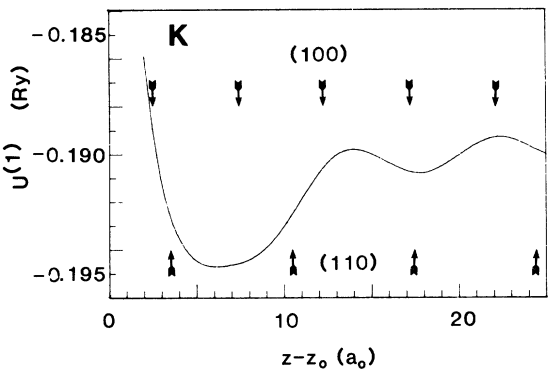

FIG. 2. Single-ion potential $U^{(1)}(z)$ for K. Layer positions are indicated by arrows.

tion, depth, and curvature—see dashed curves in Figs. 3–7) to the $M1$ model pair potentials of Dagens *et al.*,[41] which do yield rather satisfactory agreement with experimental dispersion curves.

The Lang-Kohn[30] surface electron density $\rho^0(z)$ for the three metals is shown in Fig. 1. These densities were obtained by Lagrange interpolation between the densities at the r_s values given in Ref. 30. The positions of the (100) and (110) crystalline layers, also shown in Fig. 1, are given by

$$z_l = z_0 + (l - \tfrac{1}{2})D \ , \tag{35}$$

where $z_0 = 3\pi/8k_F$ is the position of the jellium edge, and $D = (2k_F)^{-1}(6\pi^2)^{1/3}$ for the (100) layers and $D = (\sqrt{2}k_F)^{-1}(6\pi^2)^{1/3}$ for the (110) layers [the Fermi momentum k_F is related to r_s by $k_F = (9\pi/4)^{1/3}/r_s$]. The Lang-Kohn electron density enters the calculation through the first-order correction to the total energy and contributes to the E_H term in the single-ion potential, Eq. (34b). The surface electron density of the infinite barrier model[38] is also shown in Fig. 1. We have found that the use of this infinite barrier electron density in place of the Lang-Kohn density yields values of E_H which are in close quantitative agreement with the results obtained using the Lang-Kohn density, particularly for large z. We use the infinite barrier density to extend $\rho^0(z)$ to values of z larger than those provided in the tables of Ref. 18(a).

In performing the numerical integration over Q and q_z to obtain the results presented in this section we have used a grid of points in Q,q_z with spacing $\Delta Q = \Delta q_z = 0.04k_F$, and have truncated the integrals when convergence is obtained (in most cases a maximum of $q = 12k_F$ is sufficient). The derivatives of the potentials $U^{(1)}(z)$ and $U^{(2)}(R;z_1,z_2)$ which are presented in the tables were obtained numerically in each case by evaluating the quantities at points $z, z \pm 0.01D$ and $R, R \pm 0.01D$, where D is the (100) or (110) layer spacing. The units of energy and of length used in the tables are e^2k_F and k_F^{-1}, respectively, to facilitate comparison of the results for the different metals.

The single-ion-potential results are summarized in Tables II, III, and IV for Na, K, and Rb, respectively. The general behavior of $U^{(1)}$ as a function of ion position

TABLE II. Single-ion potential for Na, $U^{(1)}(z) = E_s + E_H + E^0_{BS}$ and derivatives, evaluated at the (100) and (110) layer positions $z = z_0 + (l - \frac{1}{2})D$; D is the layer spacing. The units of energy and length are, respectively, e^2k_F and k_F^{-1}, where $k_F = (9\pi/4)^{1/3}/r_s$ and r_s is given in Table I.

	1	2	3	4	5
			(100) layer		
E_s	−0.2739	−0.2697	−0.2660	−0.2648	−0.2643
E_H	0.0328	0.0356	0.0369	0.0359	0.0358
E^0_{BS}	0.0085	0.0002	0.0000	−0.0005	0.0009
$U^{(1)}$	−0.2326	−0.2338	−0.2290	−0.2294	−0.2276
$\partial E_s/\partial z$	−0.0107	0.0039	0.0008	0.0004	0.0002
$\partial E_H/\partial z$	0.0316	−0.0039	−0.0004	0.0002	−0.0005
$\partial E^0_{BS}/\partial z$	−0.0304	−0.0006	0.0026	−0.0015	0.0003
$\partial U^{(1)}/\partial z$	−0.0095	−0.0006	0.0031	−0.0009	−0.0000
$\partial^2 E_s/\partial z^2$	0.032	−0.003	−0.000	−0.000	0.000
$\partial^2 E_H/\partial z^2$	0.006	0.010	−0.002	0.000	0.000
$\partial^2 E^0_{BS}/\partial z^2$	−0.010	0.007	−0.001	0.003	−0.003
$\partial^2 U^{(1)}/\partial z^2$	−0.027	0.013	−0.003	0.003	−0.002
			(110) layer		
E_s	−0.2760	−0.2668	−0.2648	−0.2642	
E_H	0.0428	0.0365	0.0360	0.0355	
E^0_{BS}	−0.0013	−0.0015	−0.0009	−0.0002	
$U^{(1)}$	−0.2346	−0.2317	−0.2297	−0.2289	
$\partial E_s/\partial z$	−0.0008	0.0014	0.0003	0.0001	
$\partial E_H/\partial z$	0.0119	0.0016	0.0002	−0.0000	
$\partial E^0_{BS}/\partial z$	−0.0128	0.0005	−0.0013	−0.0014	
$\partial U^{(1)}/\partial z$	−0.0017	0.0035	−0.0008	−0.0013	
$\partial^2 E_s/\partial z^2$	0.017	−0.001	0.000	−0.000	
$\partial^2 E_H/\partial z^2$	−0.059	−0.003	−0.000	0.001	
$\partial E^0_{BS}/\partial z^2$	0.051	0.005	0.003	0.000	
$\partial U^{(1)}/\partial z^2$	0.009	0.001	0.003	0.001	

TABLE III. Single-ion potential for K, and derivatives. See the caption for Table II.

	1	2	3	4	5
			(100) layer		
E_s	−0.2674	−0.2633	−0.2596	−0.2585	−0.2580
E_H	0.0222	0.0167	0.0185	0.0174	0.0176
$E^0_{\rm BS}$	0.0059	0.0001	−0.0001	−0.0005	0.0007
$U^{(1)}$	−0.2393	−0.2465	−0.2413	−0.2417	−0.2398
$\partial E_s/\partial z$	−0.0119	0.0039	0.0008	0.0004	0.0002
$\partial E_H/\partial z$	0.0134	−0.0034	−0.0003	0.0004	−0.0004
$\partial E^0_{\rm BS}/\partial z$	−0.0190	0.0001	0.0022	−0.0013	0.0002
$\partial U^{(1)}/\partial z$	−0.0175	0.0006	0.0027	−0.0005	0.0001
$\partial^2 E_s/\partial z^2$	0.034	−0.003	−0.000	−0.000	0.000
$\partial^2 E_H/\partial z^2$	0.018	0.012	−0.003	0.001	0.000
$\partial^2 E^0_{\rm BS}/\partial z^2$	−0.019	−0.007	−0.000	0.002	−0.003
$\partial^2 U^{(1)}/\partial z^2$	0.032	0.002	−0.003	0.003	−0.001
			(110) layer		
E_s	−0.2698	−0.2604	−0.2585	−0.2579	
E_H	0.0277	0.0179	0.0175	0.0174	
$E^0_{\rm BS}$	−0.0020	−0.0013	−0.0006	0.0000	
$U^{(1)}$	−0.2441	−0.2438	−0.2417	−0.2404	
$\partial E_s/\partial z$	−0.0015	0.0013	0.0003	0.0001	
$\partial E_H/\partial z$	0.0066	0.0020	0.0005	0.0000	
$\partial E^0_{\rm BS}/\partial z$	−0.0128	0.0002	−0.0011	−0.0012	
$\partial U^{(1)}/\partial z$	−0.0077	0.0036	−0.0003	−0.0011	
$\partial^2 E_s/\partial z^2$	0.019	−0.001	−0.000	−0.000	
$\partial^2 E_H/\partial z^2$	−0.049	−0.002	0.000	0.000	
$\partial^2 E^0_{\rm BS}/\partial z^2$	0.047	0.004	0.003	0.000	
$\partial U^{(1)}/\partial z^2$	0.018	0.001	0.003	0.000	

TABLE IV. Single-ion potential for Rb, and derivatives. See the caption for Table II.

	1	2	3	4	5
			(100) layer		
E_s	−0.2677	−0.2633	−0.2597	−0.2586	−0.2581
E_H	0.0203	0.0113	0.0128	0.0118	0.0120
$E^0_{\rm BS}$	0.0046	−0.0002	−0.0000	−0.0005	0.0004
$U^{(1)}$	−0.2427	−0.2523	−0.2469	−0.2473	−0.2456
$\partial E_s/\partial z$	−0.0111	0.0039	0.0008	0.0004	0.0002
$\partial E_H/\partial z$	0.0060	−0.0032	−0.0005	0.0004	−0.0000
$\partial E^0_{\rm BS}/\partial z$	−0.0144	0.0006	0.0015	−0.0009	−0.0000
$\partial U^{(1)}/\partial z$	−0.0196	0.0013	0.0019	−0.0000	0.0000
$\partial^2 E_s/\partial z^2$	0.034	−0.003	−0.001	0.000	0.000
$\partial^2 E_H/\partial z^2$	0.005	0.012	−0.002	0.000	0.000
$\partial^2 E^0_{\rm BS}/\partial z^2$	−0.007	−0.006	−0.000	0.002	0.000
$\partial^2 U^{(1)}/\partial z^2$	0.032	0.003	−0.003	0.002	0.000
			(110) layer		
E_s	−0.2701	−0.2605	−0.2586	−0.2580	
E_H	0.0229	0.0124	0.0119	0.0119	
$E^0_{\rm BS}$	−0.0015	−0.0009	−0.0005	−0.0000	
$U^{(1)}$	−0.2487	−0.2490	−0.2472	−0.2461	
$\partial E_s/\partial z$	−0.0007	0.0013	0.0003	0.0001	
$\partial E_H/\partial z$	0.0023	0.0017	0.0004	0.0001	
$\partial E^0_{\rm BS}/\partial z$	−0.0112	0.0003	−0.0007	−0.0008	
$\partial U^{(1)}/\partial z$	−0.0095	0.0033	0.0001	−0.0006	
$\partial^2 E_s/\partial z^2$	0.019	−0.001	−0.000	0.000	
$\partial^2 E_H/\partial z^2$	−0.032	−0.003	−0.000	0.000	
$\partial^2 E^0_{\rm BS}/\partial z^2$	0.031	0.003	0.002	0.000	
$\partial^2 U^{(1)}/\partial z^2$	0.017	−0.001	0.002	0.000	

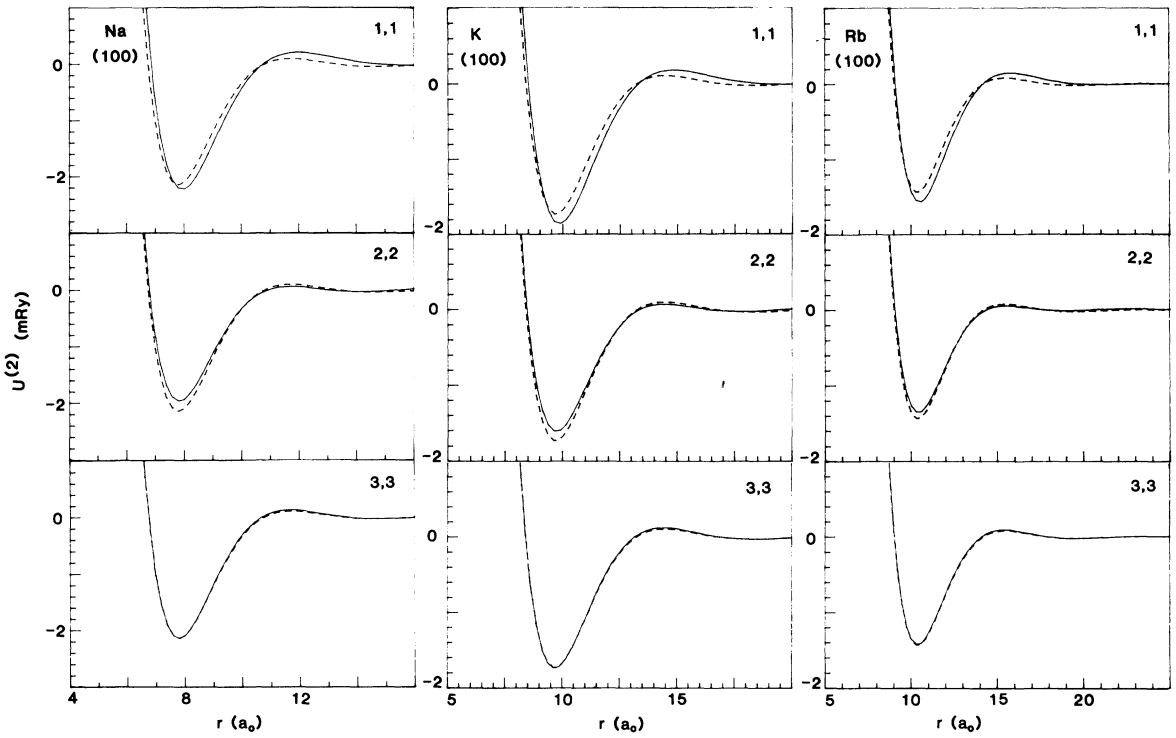

FIG. 3. Pair-interaction potentials, $U^{(2)}(R;z_1,z_2)$, for ions in the same (100) layer, plotted vs the interionic distance $r=(R^2+(z_1-z_2)^2)^{1/2}$ as R is varied and z_1,z_2 are constants. The z coordinates of the ions correspond to layer positions, $z_1=z_0+(l_1-\frac{1}{2})D$, $z_2=z_0+(l_2-\frac{1}{2})D$; the values of l_1,l_2 are indicated in the upper right-hand corner of each graph. The units of energy and length are 10^{-3} Ry and a_0 (Bohr radius), respectively.

z is shown graphically in Fig. 2, which was drawn from the values of $U^{(1)}(z)$ and its derivatives at the (100) and (110) layer positions for K.

The largest contribution to the single-ion potential $U^{(1)}$, Eq. (33), is the interaction of the ion with its own screening electron density E_s. The second largest contribution is E_H, which comes from the first-order energy and corresponds to the direct interaction of the ionic pseudopotential with the difference, $\rho^0(z)-\Omega_0^{-1}\Theta(z-z_0)$, between the Lang-Kohn electron density and a truncated bulk density. Both E_s and E_H oscillate about a constant bulk value as z increases, and the magnitude of the oscillations decreases as the distance from the surface increases. The third contribution, E_{BS}, is much smaller in magnitude and oscillates about a bulk value of zero, but the magnitude of the oscillation decreases more slowly as z increases. It is the oscillations in $U^{(1)}$ rather than the magnitude which are important in determining surface structure, since these oscillations give rise to forces on the ions normal to the surface plane. Differences in the magnitude of $U^{(1)}$ for different ionic species (evaluated for the same Ω_0) are important in determining impurity formation energies and surface concentration profiles in alloys, but this is the subject of a planned future publication and will not be discussed here.

The derivative of the single-ion potential, $\partial U^{(1)}/\partial z$, is negative for ions in the surface layer of both the (100) and (110) surfaces of each of the metals considered, corresponding to a force on the ions toward the bulk. There is a large amount of cancellation between the derivatives of the three terms E_s, E_H, and E_{BS}^0 near the surface. E_H and E_{BS}^0 are related in that E_H is a direct interaction while E_{BS}^0 is an interaction mediated by the screening electron densities, and the forces arising from these two interactions tend to cancel in the surface layer. The cancellation is almost complete for the higher electron density metal, Na. The single-ion forces on ions deeper than about the third (100) layer or second (110) layer are primarily due to oscillations in E_{BS}^0, which are in turn due to quantum interference effects in the solution for the screening electron densities.

The results of calculations of the pair-interaction potential $U^{(2)}(R,z_1,z_2)$ are summarized in Figs. 3–7 and Tables V–VIII. These interaction potentials are not two-body central-force potentials in the surface region since they depend on the z coordinates of the two ions separately. However, $U^{(2)}$ does depend on the magnitude of the ionic separation parallel to the surface, R, and we can get some feeling for how $U^{(2)}$ differs from the bulk interaction by plotting $U^{(2)}(R,z_1,z_2)$ vs $r=[R^2+(z_1-z_2)^2]^{1/2}$ as R is varied while keeping z_1 and z_2 fixed. This is done in Figs. 3–7, where z_1 and z_2 are layer positions for (100) or (110) layers. The bulk pair potential is shown as the dashed curve in each figure. For ions near the surface the minimum in the pair-interaction potential may be significantly deeper or shallower than the bulk pair-potential minimum and may be shifted to larger or smaller interionic distance r depending on the z coordinates of the two

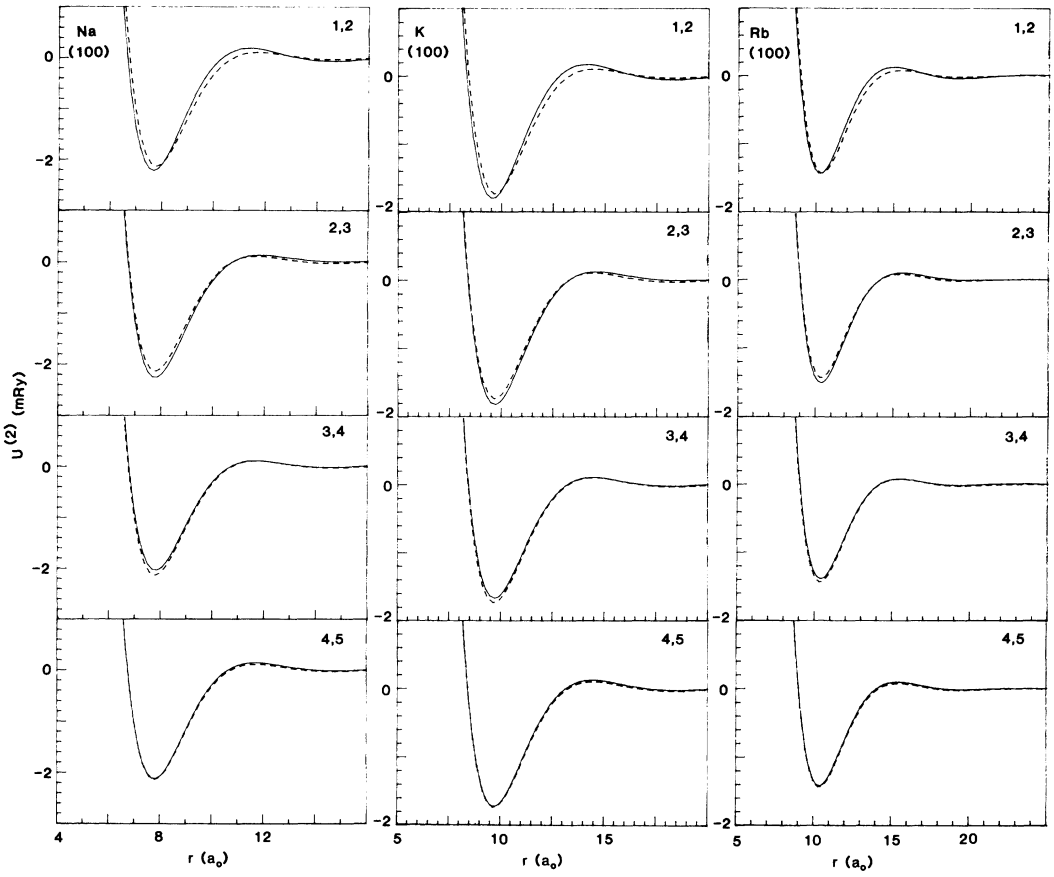

FIG. 4. Pair-interaction potentials for ions in adjacent (100) layers. See the caption for Fig. 3.

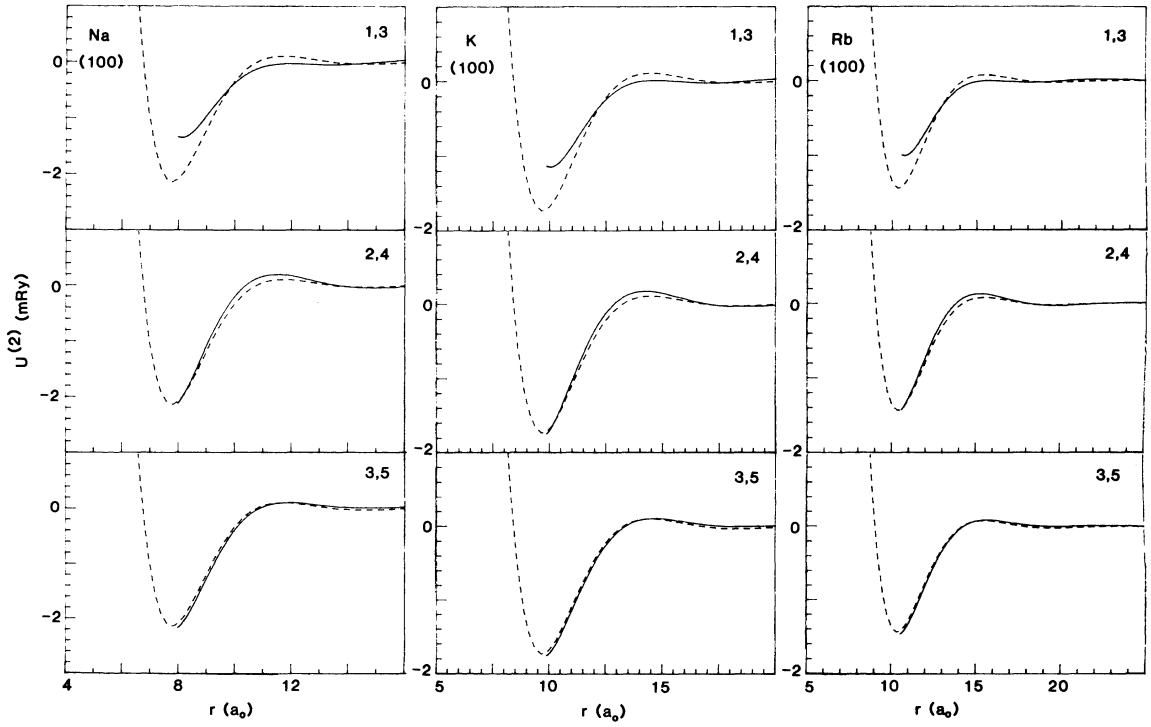

FIG. 5. Pair-interaction potentials for ions in next-nearest-neighbor (100) layers. See the caption for Fig. 3.

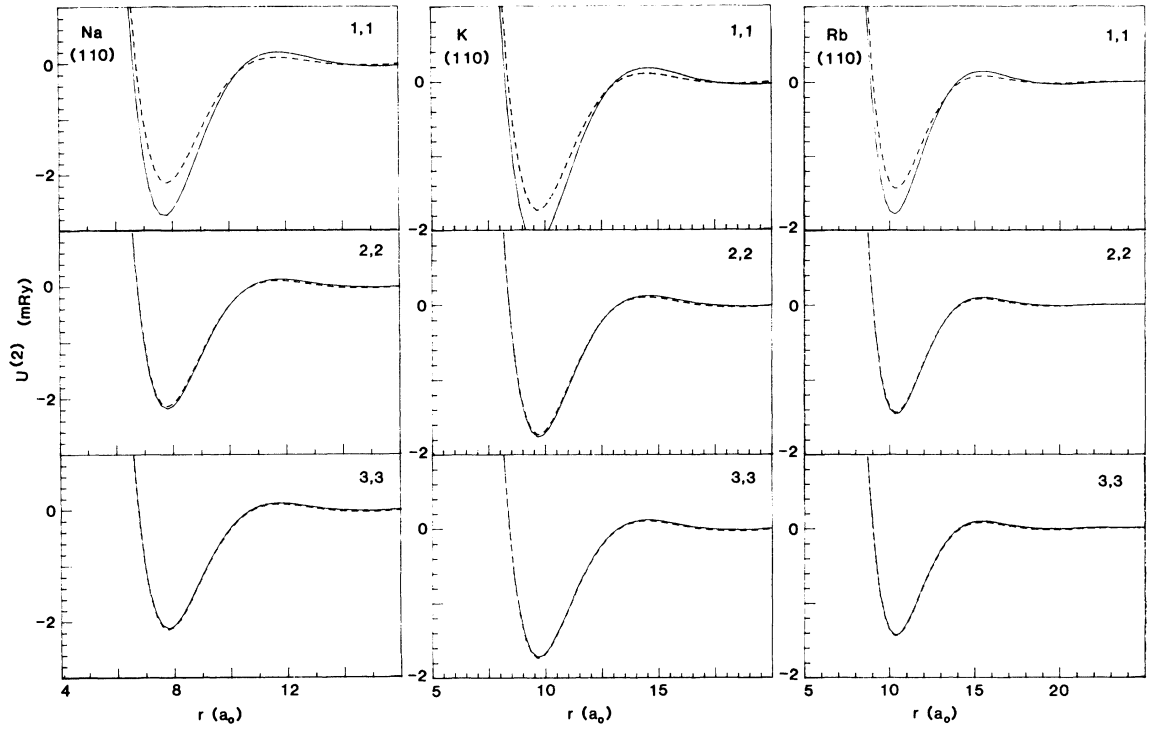

FIG. 6. Pair-interaction potentials for ions in the same (110) layers. See the caption for Fig. 3.

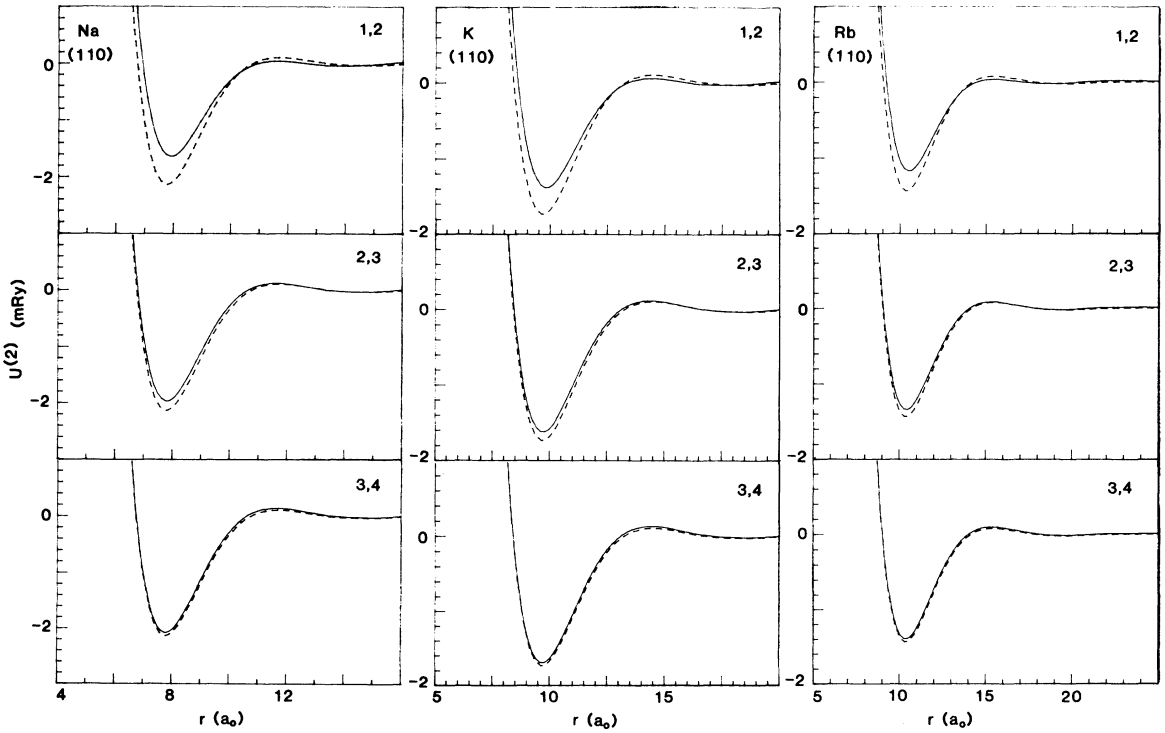

FIG. 7. Pair-interaction potentials for ions in adjacent (110) layers. See the caption for Fig. 3.

TABLE V. First derivative of the pair-interaction potential with respect to z_1, $\partial U^{(2)}(R;z_1,z_2)/\partial z_1$, for K ions in the same layer, $z_1=z_2=z_0+(l_1-\frac{1}{2})D$, evaluated for second- and third-nearest-neighbors (NN) ions in the first five (100) layers, and for first-, second-, and third-nearest-neighbor ions in the first four (110) layers. The units of energy and length are, respectively, e^2k_F and k_F^{-1}.

	1	2	3	4	5	Bulk
			(100) layer $l_1=l_2$			
Second NN	−0.001 36	−0.000 13	0.000 04	0.000 01	0.000 01	0.0
Third NN	−0.000 13	−0.000 02	0.000 00	0.000 02	0.000 01	0.0
			(110) layer $l_1=l_2$			
First NN	−0.000 21	−0.000 01	0.000 01	0.000 01		0.0
Second NN	0.000 21	0.000 01	0.000 01	0.000 01		0.0
Third NN	0.000 09	0.000 03	0.000 02	0.000 01		0.0

ions. In addition, the magnitude of the Friedel oscillations in the interaction potential as r increases may be either increased or decreased. It has been shown by Lau and Kohn[42] that the oscillatory part of the interaction between point ions adsorbed on a substrate with a spherical Fermi surface is proportional to $\cos(2k_FR)/R^5$, in contrast to the R^{-3} dependence in the bulk. We have not attempted such an asymptotic analysis, and the inclusion of quantum interference effects may alter this behavior. However, as the distance of the two ions from the surface increases, the bulk behavior must result. The interaction between ions in the same layer ($z_1=z_2$) is essentially bulklike for ions deeper than the third (100) layer, but the effect of the surface on the interaction between ions in different layers extends further, i.e., the interaction between ions in the third and fourth or third and fifth (100) layers still shows marked differences from the bulk interaction. The differences between $U^{(2)}$ and the bulk pair potential are fairly uniform for the three metals, although there is a trend toward larger differences in the higher electron density (smaller r_s) metal Na.

In order to examine the dependence of the pair-interaction potential on the z coordinates of the two ions we have calculated the first and second derivatives $\partial U^{(2)}/\partial z_1$, $\partial U^{(2)}/\partial z_2$, $\partial^2 U^{(2)}/\partial R\partial z_{1,2}$, $\partial^2 U^{(2)}/\partial^2 z_{1,2}$, and $\partial^2 U^{(2)}/\partial z_1\partial z_2$ for ions at lattice sites in the (100) and (110) layers, and compare these to the derivatives of the bulk pair potential in Tables V–VIII (for K only). The units of energy and length used in these tables are again e^2k_F and k_F^{-1}, respectively.

The fact that the pair-interaction potential is not a central-force interaction is first clearly illustrated in Table V, which gives $\partial U^{(2)}/\partial z_1=\partial U^{(2)}/\partial z_2$ for ions in the same layer ($z_1=z_2$). While in the bulk this derivative is zero, for ions in a layer near the surface it is not zero and for nearest and next-nearest neighbors it is about an order of magnitude smaller than the force due to the single-ion potential. This amounts to an additional force normal to the surface on each ion in the layer since the potential energy due to interaction between ions in the layer can be decreased by moving the entire layer. Table VI gives the derivatives $\partial U^{(2)}/\partial z_1$ and $\partial U^{(2)}/\partial z_2$ for ions in different layers. In contrast to the bulk where $\partial U^{(2)}/\partial z_1=-\partial U^{(2)}/\partial z_2$, in the surface region the derivatives with respect to z_1 and z_2 are not equal in magnitude and may not be opposite in sign [e.g., second nearest neighbors in (100) layers 1 and 3].

Table VII and VIII give the second derivatives of $U^{(2)}$ with respect to various combinations of z_1, z_2, and R. Again we see that the derivatives of the pair-interaction potential for ions in the surface region are significantly different from the derivatives of the central-force bulk

TABLE VI. First derivatives of the pair-interaction potential for K ions, $U^{(2)}(R;z_1,z_2)$, with respect to z_1 and z_2, evaluated for ions in different layers, $z_1=z_0+(l_1-\frac{1}{2})D$ and $z_2=z_0+(l_2-\frac{1}{2})D$, for first nearest neighbors (NN) in (100) layers and first and second nearest neighbors in (110) layers. The units of energy and length are, respectively, e^2k_F and k_F^{-1}.

		(1,2)	(2,3)	(3,4)	(4,5)	Bulk
				(100) layers (l_1,l_2)		
First NN	$\partial U^{(2)}/\partial_1$	0.005 86	0.005 13	0.005 09	0.005 20	0.005 13
	$\partial U^{(2)}/\partial z_2$	−0.003 59	−0.005 33	−0.005 09	−0.005 10	−0.005 13
				(110) layers (l_1,l_2)		
First NN	$\partial U^{(2)}/\partial z_1$	0.007 07	0.007 33	0.007 32		0.007 26
	$\partial U^{(2)}/\partial z_2$	−0.007 44	−0.007 06	−0.007 12		−0.007 26
Second NN	$\partial U^{(2)}/\partial z_1$	−0.000 73	−0.000 51	−0.000 49		0.000 51
	$\partial U^{(2)}/\partial z_2$	0.00012	0.00058	0.00060		−0.00051
				(100) layers (l_1,l_2)		
Second NN	$\partial U^{(2)}/\partial z_1$	−0.000 81	−0.000 66	−0.000 77		−0.000 73
	$\partial U^{(2)}/\partial z_2$	−0.000 70	0.001 32	0.000 50		0.000 73

TABLE VII. Second derivatives of the pair-interaction potential $U^{(2)}(R;z_1,z_2)$ for K ions in the same layer, $z_1=z_2=z_0+(l-\frac{1}{2})D$, evaluated for second nearest neighbors (NN) in (100) layers and for first and second nearest neighbors in (110) layers. The units of energy and length are, respectively, e^2k_F and k_F^{-1}.

		1	2	3	4	5	Bulk
				(100) layer $l_1=l_2$			
Second NN	$\partial^2U^{(2)}/\partial R\partial z_1$	0.002 11	−0.000 02	−0.000 01	0.000 00	0.000 01	0.0
	$\partial^2U^{(2)}/\partial z_1^2$	0.002 15	0.000 13	0.000 21	0.000 19	0.000 21	0.000 19
	$\partial^2U^{(2)}/\partial z_1\partial z_2$	0.003 62	−0.000 18	−0.000 21	−0.000 17	−0.000 20	−0.000 19
				(110) layer $l_1=l_2$			
First NN	$\partial^2U^{(2)}/\partial R\partial z_1$	0.001 16	0.000 01	−0.000 01	0.000 01		0.0
	$\partial^2U^{(2)}/\partial z_1^2$	−0.001 30	−0.002 63	−0.002 62	−0.002 61		−0.002 63
	$\partial^2U^{(2)}/\partial z_1\partial z_2$	0.005 30	0.002 75	0.002 65	0.002 61		0.002 63
Second NN	$\partial^2U^{(2)}/\partial R\partial z_1$	0.000 47	0.000 05	0.000 00	0.000 00		0.0
	$\partial^2U^{(2)}/\partial z_1^2$	0.001 02	0.000 21	0.000 19	0.000 19		0.000 19
	$\partial^2U^{(2)}/\partial z_1\partial z_2$	0.001 12	−0.000 12	−0.000 17	−0.000 19		−0.000 19

pair potential, and may have the opposite sign.

The results presented in Tables V–VIII support the conclusions stated earlier in the discussion of the figures that (a) the pair-interaction potential in the surface region is significantly different from the bulk central-force pair potential, (b) the effect of the surface on the interaction between ions in different layers (different z coordinates) extends further than the effect on the interaction between ions in the same layer, and (c) in any case, the interaction between pairs of ions both of which are deeper than about the fourth (100) or third (110) layer positions is essentially bulk like. The major differences of $U^{(2)}$ from the bulk pair potential are due to quantum interference effects in the solutions for the screening electron density, the terms $u_1(\vec{q})$ and $u_\sigma(\vec{q})$ in Eq. (19). If these quantum interference terms are simply set equal to zero only the interaction between pairs of ions very close to the surface [the (100) surface layer] deviate from the bulk interaction. In the semiclassical limit (mentioned in Sec. II B) the quantum interference terms do not occur, but the position of the jellium edge is $z_0=0$, so the effect of the surface on the pair-interaction potential in the semiclassical response model might extend somewhat further. However, the semiclassical response model restricts the choice of ionic pseudopotential since there is no response of the electron gas for $z\leq 0$, and therefore the positive charge density which gives rise to the ionic pseudopotential must not extend past the jellium edge (see Appendix C).

The single-ion and pair-interaction potentials derived in Sec. II C and discussed in this section are, in principle, sufficient to treat problems involving surface relaxation,[43] defect energies, and surface segregation in alloys. Howev-

TABLE VIII. Second derivatives of the pair-interaction potential $U^2(R;z_1,z_2)$, for K ions in adjacent layers, $z_1=z_0+(l_1-\frac{1}{2})D$ and $z_2=z_0+(l_2-\frac{1}{2})D$ with $l_2=l_1+1$, evaluated for first nearest neighbors (NN) in (100) layers and for first and second nearest neighbors in (110) layers. The units of energy and length are, respectively, e^2k_F and k_F^{-1}.

		(1,2)	(2,3)	(3,4)	(4,5)	Bulk
				(100) layers (l_1,l_2)		
First NN	$\partial^2U^{(2)}/\partial R\partial z_1$	−0.017 06	−0.016 18	−0.016 30	−0.016 38	−0.016 29
	$\partial^2U^{(2)}/\partial R\partial z_2$	0.015 51	0.016 54	0.016 22	0.016 34	0.016 29
	$\partial^2U^{(2)}/\partial z_1^2$	0.008 86	0.009 02	0.008 80	0.008 92	0.008 88
	$\partial^2U^{(2)}/\partial z_1\partial z_2$	−0.010 22	−0.008 69	−0.008 93	−0.008 92	−0.008 88
	$\partial^2U^{(2)}/\partial z_2^2$	0.008 85	0.009 18	0.008 68	0.009 00	0.008 88
				(110) layers (l_1,l_2)		
First NN	$\partial^2U^{(2)}/\partial R\partial z_1$	−0.016 39	−0.016 41	−0.016 35		−0.016 29
	$\partial^2U^{(2)}/\partial R\partial z_2$	0.015 94	0.016 12	0.016 23		0.016 29
	$\partial^2U^{(2)}/\partial z_1^2$	0.020 13	0.020 37	0.020 44		0.020 41
	$\partial^2U^{(2)}/\partial z_1\partial z_2$	−0.020 69	−0.020 54	−0.020 48		−0.020 41
	$\partial^2U^{(2)}/\partial z_2^2$	0.018 29	0.020 01	0.020 43		0.020 41
Second NN	$\partial^2U^{(2)}/\partial R\partial z_1$	−0.003 97	−0.004 06	−0.004 05		−0.003 99
	$\partial^2U^{(2)}/\partial R\partial z_2$	0.003 87	0.003 86	0.003 94		0.003 99
	$\partial^2U^{(2)}/\partial z_1^2$	0.004 19	0.004 14	0.004 17		0.004 18
	$\partial^2U^{(2)}/\partial z_1z_2$	−0.004 20	−0.004 23	−0.004 22		−0.004 18
	$\partial^2U^{(2)}/\partial z_2^2$	0.003 14	0.003 86	0.004 13		0.004 18

er, due to the long-range nature of the pair interactions and the fact that in the surface region they are not two-body central-force potentials, a real-space approach to such problems is cumbersome. Calculations using a reciprocal-space approach to minimize the total energy and determine the relaxed surface structure are reported elsewhere,[17,18(a)] and surface segregation and defect energetics will be treated in planned future publications.

The model as developed here is not directly applicable to surface vibrations because the use of the jellium system as a starting point and the infinite barrier response model specifies the location and orientation of the surface plane with respect to the coordinate system; thus the dynamical matrix obtained from this model would not satisfy the condition of rotational invariance. It is clear, however, that two-body central-force potentials are not sufficient to describe the interionic interactions in the surface region and that the interaction of the ions with the inhomogeneous electron gas, which is the origin of the single-ion potentials, must be included. It may be possible to impose rotational invariance and obtain and approximate dynamical matrix.[44] The single-ion and pair-interaction potentials can be used in Monte Carlo or molecular-dynamics simulations. Monte Carlo studies on liquid-metal surfaces[45] have shown that the inclusion of a single-ion potential leads to stable density oscillations at the surface.

In summary, we have developed a formulation based on the use of ionic pseudopotentials and linear-response theory which is applicable to problems involving minimization of the surface energy of a simple metal with respect to ionic species and/or position. The formulation maintains the full three-dimensional nature of the system and does not require crystalline order; thus it is possible to treat defects near the surface and random alloys as well as ideal surfaces. We have decomposed the total-energy expression into a density-dependent term and real-space single-ion and pair-interaction potentials. An examination of these potentials shows that both the single-ion potentials and the non-central-force nature of the pair-interaction potentials are important in surface structure and energetics and in surface lattice virbations of simple metals.

ACKNOWLEDGMENT

This work was supported by the U. S. Department of Energy under Contract No. EG-S-05-5489.

APPENDIX A

In this appendix Eq. (12) for the Fourier transform of the symmetrized screening electron density is derived. Substituting Eq. (6a) into Eq. (11b) and using the fact that $\alpha_0(|\vec{R}-\vec{R}'|;z,z')$ vanishes for negative z' gives

$$\rho_{is}(\vec{q})=2\int d^2R\, e^{i\vec{Q}\cdot\vec{R}}\int_0^\infty dz\cos(q_z z)\int d^2R'\int_0^\infty dz'\alpha_0(|\vec{R}-\vec{R}'|;z,z')[w_i(\vec{r}')+\phi_i(\vec{r}')]\ . \tag{A1}$$

When the integrals over $\vec{R}$ and $\vec{R}'$ are performed we obtain

$$\rho_{is}(\vec{q})=2\int_0^\infty dz'[w_i(Q,z')+\phi_i(Q,z')]\int_0^\infty dz\cos(q_z z)\alpha_0(Q;z,z')\ . \tag{A2}$$

The integral over z in Eq. (A2) is evaluated using Eq. (10) for $\alpha_0(Q;z,z')$ and the integral representation of the Dirac δ function

$$\pi\delta(k)=1+\int_0^\infty dz\cos(kz)\ .$$

The result is

$$\int_0^\infty dz\cos(q_z z)\alpha_0(Q;z,z')=\frac{1}{\pi}\int d\kappa\sin(\kappa z')\int d\kappa'\sin(\kappa' z')\mathscr{L}(Q;\kappa,\kappa')$$
$$\times[\delta(q_z+\kappa-\kappa')+\delta(q_z-\kappa+\kappa')-\delta(q_z+\kappa+\kappa')-\delta(q_z-\kappa-\kappa')]\ . \tag{A3}$$

From the definition of the two-dimensional RPA response function, Eq. (8b), it is clear that $\mathscr{L}(Q;\kappa,\kappa')$ is invariant to transformations which interchange κ and κ' or change the sign of κ,κ', or both:

$$\mathscr{L}(Q;\kappa,\kappa')=\mathscr{L}(Q;\kappa,-\kappa')=\mathscr{L}(Q;\kappa',\kappa)\ .$$

These symmetry properties are used together with the fact that κ and κ' are to be integrated over both positive and negative values to obtain

$$\int_0^\infty dz\cos(q_z z)\alpha_0(Q;z,z')=\pi^{-1}\int d\kappa\,\mathscr{L}(Q;\kappa+q_z/2,\kappa-q_z/2)[\cos(q_z z')-\cos(2\kappa z')]\ . \tag{A4}$$

We now substitute Eq. (A4) back into Eq. (A2) and evaluate the integral over z'. The result is Eq. (12) of the text:

$$\rho_{is}(\vec{q})=\alpha_0(q)[w_{is}(\vec{q})+\phi_{is}(\vec{q})]-\pi^{-1}\int d\kappa\,\mathscr{L}(Q;\kappa+q_z/2,\kappa-q_z/2)[w_{is}(Q,2\kappa)+\phi_{is}(Q,2\kappa)]\ , \tag{A5}$$

where

$$\alpha_0(q)=\pi^{-1}\int d\kappa\,\mathscr{L}(Q;\kappa+q_z/2,\kappa-q_z/2)$$

is the RPA response function for an infinite system.

APPENDIX B

In this appendix we derive Eq. (16) for the Fourier transform of the self-consistent effective potential due to the screening electron density in the symmetrized system. From Eq. (6b) and the definition of the symmetrized system we have

$$\phi_{is}(\vec{r})=\int d^3r' g(\vec{r},\vec{r}')v_C(|\vec{r}-\vec{r}'|)\rho_{is}(\vec{r}')[1-\Theta(z)\Theta(-z')-\Theta(-z)\Theta(z')] , \tag{B1}$$

where $g(\vec{r},\vec{r}')=1-G(\vec{r},\vec{r}')$ and $G(\vec{r},\vec{r}')$ is the local-field correction discussed in the text. The Fourier transform of Eq. (B1) is

$$\begin{aligned}\phi_{is}(\vec{q})=&\,v_C(q)\rho_{is}(\vec{q})-\int d^3r\, e^{i\vec{q}\cdot\vec{r}}\int d^3r' G(\vec{r},\vec{r}')v_C(|\vec{r}-\vec{r}'|)\rho_{is}(\vec{r}')\\&-\int d^3r\, e^{i\vec{q}\cdot\vec{r}}\int d^3r' v_C(|\vec{r}-\vec{r}'|)\rho_{is}(\vec{r}')[\Theta(z)\Theta(-z')+\Theta(-z)\Theta(z')]\\&+\int d^3r\, e^{i\vec{q}\cdot\vec{r}}\int d^3r' G(\vec{r},\vec{r}')v_C(|\vec{r}-\vec{r}'|)\rho_{is}(\vec{r}')[\Theta(z)\Theta(-z')+\Theta(-z)\Theta(z')] .\end{aligned} \tag{B2}$$

Owing to translational invariance in the x-y plane, $G(\vec{r},\vec{r}')=G(|\vec{R}-\vec{R}'|;z,z')$; thus the remaining integrals over $\vec{R}$ and $\vec{R}'$ in Eq. (B2) result in two-dimensional Fourier transforms of the functions G, v_C, and ρ_{is}. If, as discussed in the text, we make the assumption that $G(\vec{r},\vec{r}')=G(|\vec{r}-\vec{r}'|)$ the second term in the rhs of Eq. (B2) becomes

$$-\int d^3r\, e^{i\vec{q}\cdot\vec{r}}\int d^3r' G(|\vec{r}-\vec{r}'|)v_C(|\vec{r}-\vec{r}'|)\rho_{is}(\vec{r}')=-G(q)v_C(q)\rho_{is}(\vec{q}) . \tag{B3}$$

To evaluate the third term on the rhs of Eq. (B2) we use the identity

$$v_C(r)=\frac{e^2}{r}=\frac{e^2}{2\pi}\int\frac{d^2K}{K}\exp(-i\vec{K}\cdot\vec{R}-K|z|)$$

and substitute the inverse Fourier transform of $\rho_{is}(\vec{k})$ for $\rho_{is}(\vec{r}')$ to get

$$\begin{aligned}&-\int d^3r\, e^{i\vec{q}\cdot\vec{r}}\int d^3r' v_C(|\vec{r}-\vec{r}'|)\rho_{is}(\vec{r}')[\Theta(z)\Theta(-z')+\Theta(-z)\Theta(z')]\\&=-\frac{2\pi e^2}{Q}\int dk_z\rho_{is}(Q,k_z)\int dz\, e^{iq_z z}\int dz' e^{-ik_z z'}[\Theta(z)\Theta(-z')+\Theta(-z)\Theta(z')]e^{-Q|z-z'|}\\&=-\frac{2\pi e^2}{Q}\int dk_z\rho_{is}(Q,k_z)\left[\int_0^\infty dz\, e^{(iq_z-Q)z}\int_{-\infty}^0 dz'\exp[(-ik_z+Q)z']+\int_{-\infty}^0 dz\, e^{(iq_z+Q)z}\int_0^\infty dz'\exp[(-ik_z-Q)z']\right]\\&=-\frac{2\pi e^2}{Q}\int dk_z\rho_{is}(Q,k_z)\frac{-k_zq_z+Q^2}{(k_z^2+Q^2)(q_z^2+Q^2)} .\end{aligned} \tag{B4}$$

Since $\rho_{is}(Q,k_z)$ is an even function of k_z,

$$\int dk_z\rho_{is}(Q,k_z)\frac{k_z}{k_z^2+Q^2}=0$$

and

$$\begin{aligned}-\frac{2\pi e^2}{Q}\int dk_z\rho_{is}(Q,k_z)&\frac{-k_zq_z+Q^2}{(k_z^2+Q^2)(q_z^2+Q^2)}\\&=-\frac{4\pi e^2}{q^2}\frac{1}{2\pi}\int dk_z\rho_{is}(Q,k_z)\frac{Q}{Q^2+k_z^2}\\&=v_C(q)\sigma_i(Q) ,\end{aligned} \tag{B5}$$

where $v_C(q)=4\pi e^2/q^2$ and

$$\sigma_i(Q)=-\frac{Q}{2\pi}\int dq_z\frac{\rho_{is}(\vec{q})}{q^2} . \tag{B6}$$

It is also evident that

$$\begin{aligned}\lim_{Q\to0}\sigma_i(Q)&=\lim_{Q\to0}\frac{Q}{2\pi}\int dq_z\frac{\rho_{is}(\vec{q})}{q^2}\\&=-\tfrac{1}{2}\rho_{is}(\vec{q}=\vec{0}) .\end{aligned} \tag{B7}$$

$\rho_{is}(\vec{q}=\vec{0})$ is the integrated screening electron density induced by the potential $w_{is}(\vec{r})$ and is equal to the amount of positive charge (in units of the electron charge e) which gives rise to the potential, i.e., $\rho_{is}(\vec{q}=\vec{0})=0$, since $w_i(\vec{r})$ is a neutral perturbation due to the replacement of part of the jellium positive background by the ionic pseudopotential.

The last term in Eq. (B2) is

$$\begin{aligned}X_i(\vec{q})=&\int d^3r\, e^{i\vec{q}\cdot\vec{r}}\int d^3r' G(\vec{r},\vec{r}')v_C(|\vec{r}-\vec{r}'|)\rho_{is}(\vec{r}')\\&\times[\Theta(z)\Theta(-z')+\Theta(-z)\Theta(z')] .\end{aligned} \tag{B8}$$

We do not attempt to evaluate this term here. It is not possible to reduce $X_i(\vec{q})$ to a form similar to $v_C(q)\sigma_i(Q)$, i.e., the Coulomb potential multiplying some function which is independent of q_z. Thus this term prevents the reduction of the problem of solving for $\rho_i(\vec{r})$ to the solution of a single-integral equation. However, $X_i(\vec{q})$ is negligible because, as discussed in the text, $G(\vec{r},\vec{r}')$ is very short ranged and because $\rho_{is}(\vec{r})$ vanishes at $z=0$.

APPENDIX C

In this appendix we derive Eqs. (25) and (26) which give the Fourier transforms of the symmetrized potentials

$\tilde{w}_{is}(\vec{r})$ and $V_{+s}(\vec{r})$. The definition of $\tilde{w}_{is}(\vec{r})$ can be written as

$$\tilde{w}_{is}(\vec{r})=Z(\beta_i)^{-1}[\,V_p(\beta_i;\,|\,\vec{r}-(\vec{R}_i,z_i)\,|\,)\Theta(z) + V_p(\beta_i;\,|\,\vec{r}-(\vec{R}_i,-z_i)\,|\,)\Theta(-z)]\,, \tag{C1}$$

where $\vec{r}_i=(\vec{R}_i,z_i)$ is the ion position, $Z(\beta_i)$ is the charge in units of e, β_i designates species, and $V_p(\beta_i;r)$ is the local-model pseudopotential for ionic species β_i. For notational convenience in the following we will omit the specification of ionic species.

From Eq. (24) we have

$$\tilde{w}_{is}(\vec{q})=2Z^{-1}\int_0^{L+z_0}dz\cos(q_z z)\int d^2R\,e^{i\vec{Q}\cdot\vec{R}}V_p([R^2+(z-z_i)^2]^{1/2})\,, \tag{C2}$$

where $L=\Omega^{1/3}$ is the thickness of the semi-infinite metal (the limit $L\to\infty$ will be taken) and z_0 is the distance of the jellium edge from the $z=0$ plane. Substitution of the inverse Fourier transform of $V_p(k)$ for $V_p(r)$ yields

$$\tilde{w}_{is}(\vec{q})=\frac{Z^{-1}}{2\pi}\int dk_z e^{ik_z z_i}V_p(Q,k_z)\int_0^{L+z_0}dz\,e^{-ik_z z}2\cos(q_z z)\,. \tag{C3}$$

The integral over z in Eq. (C3) is

$$2\int_0^{L+z_0}dz\exp[-ik_z(z-z_i)]\cos(q_z z)=\frac{i}{k_z+q_z}\{\exp[-ik_z(L+z_0-z_i)]\exp[-iq_z(L+z_0)]-e^{ik_z z_i}\} + \frac{i}{k_z-q_z}\{\exp[-ik_z(L+z_0-z_i)]\exp[iq_z(L+z_0)]-e^{ik_z z_i}\}\,. \tag{C4}$$

We will now express the ionic pseudopotential as

$$V_p(q)=-\frac{4\pi e^2}{q^2}Z\rho^I(q)\,, \tag{C5}$$

where $Ze\rho^I(q)$ is the Fourier transform of a spherically symmetric positive charge density which gives rise to the local pseudopotential. An obvious restriction is that $\rho^I(\,|\,\vec{r}-\vec{r}_i\,|\,)=0$ for $z-z_i<0$; or, in the case of the simplified Heine-Abarenkov potential which we use, $r_c\le z_i$, where r_c is the core radius [see Eq. (4)].

Equations (C4) and (C5) are substituted into Eq. (C3) to obtain

$$\tilde{w}_{is}(\vec{q})=\frac{1}{2\pi}\int dk_z[-4\pi e^2\rho^I(Q,k_z)]\frac{1}{2Q}\left[\frac{1}{k_z-iQ}-\frac{1}{k_z+iQ}\right] \times\left[\frac{1}{k_z+q_z}\{\exp[-ik_z(L+z_0-z_i)]\exp[-iq_z(L+z_0)]-e^{ik_z z_i}\} + \frac{1}{k_z-q_z}\{\exp[-ik_z(L+z_0-z_i)]\exp[iq_z(L+z_0)]-e^{ik_z z_i}\}\right]. \tag{C6}$$

The integral over k_z in Eq. (C6) is done by contour integration, using contours which avoid the poles on the real axis at $k_z=\pm q_z$ and which close around either the upper or lower half-planes as required by the exponents. The result of this integration is

$$\tilde{w}_{is}(\vec{q})=\frac{4\pi e^2}{q^2}\rho^I(q)2\cos(q_z z_i)+\frac{4\pi e^2}{q^2}\rho^I(Q,iQ)e^{-Qz_i} + \lim_{L\to\infty}\frac{4\pi e^2}{q^2}\rho^I(Q,-iQ)\left[\frac{q_z}{Q}\sin[q_z(L+z_0)]-\cos[q_z(L+z_0)]\right]\exp[-Q(L+z_0-z_i)]\,. \tag{C7}$$

Now $\rho^I(q)=\rho^I[(Q^2+q_z^2)^{1/2}]$, and thus $\rho^I(Q,\pm iQ)=\rho^I(q=0)$ (a more rigorous proof of this identity is possible but will not be given here), and $\rho^I(q=0)=1$ since the ionic charge Ze is factored out of the definition, Eq. (C5).

In the limit $L\to\infty$ the last term in Eq. (C7) vanishes for $Q\neq 0$ due to the exponent. For $Q=0$ the only contributions to an integral over q_z involving this term as part of the integrand are at $q_z=0$ and at any poles due to other terms in the integrand. To evaluate such integrals, which occur in the single-ion potentials, it is useful to note the physical significance of the second and third terms of the rhs of Eq. (C7). In writing Eq. (C2) we have assumed an infinite periodic system with period $2(L+z_0)$ in the z direction, which is symmetric about both $z=0$ and $z=L+z_0$. The second term on the rhs of Eq. (C7) represents the potential due to a two-dimensional density at $z=0$ which cancels the interaction between the negative and positive z parts of the periodic system, and the third term does the same at $z=L+z_0$, so that $\tilde{w}_{is}(\vec{r})=\tilde{w}_i(\vec{r})$ for $0\le z\le L+z_0$. Thus, while these terms may contribute to the $(Q=0,q_z)$ integrals involved in the single-ion potentials, their contribution is independent of the ionic posi-

tion and is in fact canceled by similar terms arising from the subtraction of the positive background potential.

The positive background potential $V_+(\vec{r})$ is given by

$$V_+(\vec{r})=i\int d^3r'\Omega_0^{-1}\Theta(z'-z_0)e^2/|\vec{r}-\vec{r}'|\ , \qquad \text{(C8)}$$

where Ω_0 is the volume per electron in the bulk of the semi-infinite system. The symmetrized Fourier transform can be obtained from the expression on the rhs of Eq. (C7) by replacing $\rho^{pp}(q)$ with Ω_0^{-1} [the Fourier transform of $\Omega_0^{-1}\delta(\vec{r})$] and integrating over the space occupied by the positive background density. The result of this operation is

$$V_{+s}(\vec{q})=(2\pi)^2\Omega_0^{-2/3}\delta(\vec{Q})v_{+s}(q_z)\ , \qquad \text{(C9)}$$

where $v_{+s}(q_z)$ is given by

$$v_{+s}(q_z)=-\frac{4\pi e^2}{q_z^2}\Omega_0^{-1/3}[2\pi\delta(q_z)-2\sin(q_z z_0)/q_z]$$
$$+\lim_{L\to\infty}\frac{4\pi e^2}{q_z^2}\Omega_0^{-1/3}L\left[1-\left[\frac{q_z}{Q}\sin[q_z(L+z_0)]-\cos[q_z(L+z_0)]\right]\right]\ . \qquad \text{(C10)}$$

The part of Eq. (C10) which depends on the system size L does not contribute to the single-ion potentials [see the discussion following Eq. (C7)].

*Permanent address: Institute of Physics, University of Mexico, Mexico 20, D. F., Mexico.

[1]Walter A. Harrison, *Pseudopotentials in the Theory of Metals* (Benjamin, Reading, Mass., 1966).

[2]For a review, see V. Heine and D. Weaire, in *Solid State Physics,* edited by H. Ehrenreich, F. Seitz, and D. Turnball (Academic, New York, 1970), Vol. 24, p. 249; see also P. K. Lam and M. L. Cohen, Phys. Rev. B 24, 4244 (1981).

[3]See A. A. Maradudin, E. W. Montroll, G. H. Weiss, and I. P. Ipatova, *Theory of Lattice Dynamics in the Harmonic Approximation* (Academic, New York, 1971); for a recent first principles calculation of phonon frequencies in Al, see P. K. Lam and M. L. Cohen, Phys. Rev. B 25, 6139 (1982).

[4]U. Landman, R. N. Hill, and M. Mostoller, Phys. Rev. B 21, 448 (1980); R. N. Barnett, C. L. Cleveland, and U. Landman, Bull. Am. Phys. Soc. 27, 210 (1982).

[5]For a review, see N. G. Lang, in *Solid State Physics,* edited by H. Ehrenreich, F. Seitz, and D. Turnbull (Academic, New York, 1973), Vol. 28, p. 225; S. C. Ying, in *Theory of Chemisorption,* edited by J. R. Smith (Springer, New York, 1980), p. 3; O. Gunnarson, in *Electrons in Disordered Metals and at Metallic Surfaces,* edited by P. Phariseau, B. L. Gyorffy, and L. Scheire (Plenum, New York, 1979), p. 1.

[6]See, e.g., V. Sahni, J. P. Perdew, and J. Gruenbaum, Phys. Rev. B 23, 6512 (1981); K.-P. Bohnen and S. C. Ying, Phys. Rev. B 22, 1806 (1980).

[7]See articles in *Solid State Physics,* edited by H. Ehrenreich, F. Seitz, and D. Turnbull (Academic, New York, 1980), Vol. 35; for application to surface vibrations, see M. Mostoller and U. Landman, Phys. Rev. B 20, 1755 (1979); J. E. Black, B. Laks, and D. L. Mills, *ibid.* 22, 1818 (1980).

[8]D. H. Lee and J. D. Joannopoulos, Phys. Rev. B 23, 4988 (1981); 23, 4997 (1981).

[9]For a review, see Joel A. Appelbaum and D. R. Hamann, Rev. Mod. Phys. 48, 496 (1976) and references therein; see also F. J. Arlingham, J. G. Gray, and J. R. Smith, in *Theory of Chemisorption,* edited by J. R. Smith (Springer, New York, 1980); M. T. Yin and M. L. Cohen, Phys. Rev. B 24, 2303 (1981).

[10]J. P. Perdew, Phys. Rev. B 25, 6291 (1982).

[11]G. P. Alldredge and L. K. Kleinman, J. Phys. F 4, L207 (1974).

[12]K. P. Bohnen, Surf. Sci. 115, L96 (1982), and references therein.

[13]R. N. Barnett, C. L. Cleveland, and U. Landman, Appl. Surf. Sci. 11/12, 703 (1982).

[14]For an approximate, semiclassical treatment, see Mark Mostoller and Mark Rasolt, Phys. Lett. 88A, 93 (1982).

[15]N. D. Lang, Phys. Rev. B 4, 4234 (1971); N. D. Lang and W. Kohn, *ibid.* 3, 1215 (1970); see also Ref. 18(a).

[16]P. Wynblatt and R. C. Ku, in *Interfacial Segregation,* edited by W. C. Johnson and J. M. Blakely (American Society of Metals, Metals Park, Ohio, 1979), p. 115, and other articles in this book.

[17]R. N. Barnett, U. Landman, and C. L. Cleveland, Phys. Rev. B 27, 6534 (1983).

[18](a) R. N. Barnett, U. Landman, and C. L. Cleveland, following paper, Phys. Rev. B 28, 1685 (1983); (b) Bull. Am. Phys. Soc. 26, 427 (1981).

[19]D. L. Price, K. S. Singwi, and M. P. Tosi, Phys. Rev. B 2, 2983 (1970).

[20]S. K. Sarkar and D. Sen, J. Phys. F 11, 377 (1981); D. Sen and S. K. Sarkar, Phys. Rev. B 22, 1856 (1980).

[21]N. W. Ashcroft, J. Phys. C 1, 232 (1968).

[22]Walter A. Harrison and John M. Wills, Phys. Rev. B 25, 5007 (1982).

[23]M. Manninen, P. Jena, R. M. Nieminen, and J. K. Lee, Phys. Rev. B 24, 7057 (1981).

[24]David D. Ling and G. D. Gelatt, Jr., Phys. Rev. B 22, 557 (1980).

[25]Z. D. Popovic, J. P. Carbotte, and G. R. Piercy, J. Phys. F 4, 351 (1974).

[26]G. Jacucci, Roger Taylor, A. Tennenbaum, and N. van Doan, J. Phys. F 11, 793 (1981).

[27]A. Rahman, Phys. Rev. A 9, 1667 (1974).

[28]I. Ebbsjö, T. Kinell, and I. Waller, J. Phys. C 13, 1865 (1980).

[29]G. Jacucci, M. L. Klein, and R. Taylor, Solid State Commun. 19, 657 (1976).

[30]N. D. Lang and W. Kohn, Phys. Rev. B 1, 4555 (1970).

[31]K. S. Singwi, A. Sjölander, M. P. Tosi, and R. H. Land, Phys.

Rev. B 1, 1044 (1970).
[32]Peter W. Lert and John H. Weare, J. Phys. C 11, 1865 (1978).
[33]D. E. Beck, V. C. Celli, G. loVeccio, and A. Magnaterra, Nuovo Cimento B 68, 230 (1970).
[34]D. M. Newns, Phys. Rev. B 1, 3304 (1970).
[35]J. Rudnick, Phys. Rev. B 5, 2863 (1972).
[36]See, e.g., John H. Rose and J. F. Dobson, Solid State Commun. 37, 91 (1981); M. Hasegawa and M. Watabe, J. Phys. C 15, 353 (1982); Peter W. Lert and John H. Weare, J. Chem. Phys. 68, 5010 (1978).
[37]J. A. Appelbaum and D. R. Hamann, Phys. Rev. B 6, 2166 (1972).
[38]J. Hubbard, Proc. R. Soc. London, Ser. A 240, 539 (1957).
[39]J. Lindenhard, K. Dan. Vidensk. Selsk. Mat. Fys. Medd. 28, 8 (1954).
[40]T. Li, X. Sun, and G.-W. Woo, Phys. Rev. B 22, 3230 (1980); J. Shen, L. Lin, L. Yu, and C.-W. Woo, Mol. Cryst. Liq. Cryst. (in press).
[41]L. Dagens, M. Rasolt, and R. Taylor, Phys. Rev. B 11, 2726 (1975); M. Rasolt and R. Taylor, *ibid.* 11, 2717 (1975).
[42]K. H. Lau and W. Kohn, Surf. Sci. 75, 69 (1982).
[43]See, e.g., H. L. Davis, J. R. Noonan, and L. H. J. Jenkins, Surf. Sci. 83, 559 (1979); D. L. Adams and U. Landman, Phys. Rev. B 15, 3775 (1977); M. A. van Hove, Surf. Sci. 80, 1 (1979); A recent low-energy electron diffraction study of the Al(110) surface showing multilayer relaxation is H. B. Nielsen, J. N. Andersen, L. Petersen, and D. L. Adams (unpublished).
[44]Giorgio Benedek, Surf. Sci. 61, 603 (1976).
[45]Mark P. D'Evelyn and Stuart A. Rice, Phys. Rev. Lett. 47, 1844 (1981).